Future Circular Collider

PUBLICATION

Simulation and tracking studies for a drift chamber at the FCC-ee experiment

Alipour Tehrani, Niloufar (CERN) *et al.*

11 April 2019

The research leading to this document is part of the Future Circular Collider Study

The electronic version of this FCC Publication is available
on the CERN Document Server at the following URL :
<http://cds.cern.ch/record/2670936>

10 April 2019
niloufar.alipour.tehrani@cern.ch

Simulation and tracking studies for a drift chamber at the FCC-ee experiment

Niloufar Alipour Tehrani
on behalf of the FCC collaboration

Summary

The physics aims at the electron-positron option for the Future Circular Collider (FCC-ee) [6], impose high precision requirements on the vertex and tracking detectors. The detector has also to match the experimental conditions such as the collisions rate and the presence of beam-induced backgrounds. A light weight tracking detector is under investigation for the IDEA (International Detector for Electron-Positron Accelerator) detector concept and consists of a drift chamber. Simulation studies of the drift chamber using the FCCSW (FCC software) are presented. Full simulations are used to study the effect of beam-induced backgrounds on this detector. Tracking for the drift chamber of the IDEA detector is also investigated using the Hough transformation method. A technical documentation on running the different software components is as well provided.

Contents

1 Introduction

The FCC-ee high-luminosity circular electron-positron collider, with center-of-mass energies $\sqrt{s}$ from 91.2 GeV to 365 GeV, allows for high-precision measurements of the properties of the Z, the W, the top quark and the Higgs boson. As a predecessor of a new 100 TeV proton-proton collider, the FCC-ee collider is foreseen to be placed in a 100 km tunnel in Geneva area as shown in Fig. 1.

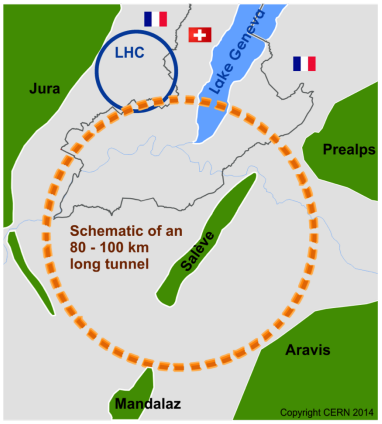

Figure 1: A possible realization of the FCC experiment near the Geneva region.

The IDEA detector, one of the two detector concepts under development for FCC-ee, has demanding requirements to match the experimental conditions. Its main components consist of: an ultra-light silicon-based vertex detector, an ultra-light drift chamber for track reconstruction and particle identification, a dual-readout calorimeter, a 2 T axial magnetic field and an instrumented return yoke as illustrated in Fig. 2. The drift chamber is being investigated using GEANT4-based simulations. Its performance and the effect of beam-induced backgrounds are presented here-below.

2 Drift chamber

The drift chamber (DCH) is optimized to provide excellent tracking, high precision momentum measurement and excellent particle identification using cluster counting technique with an extremely low material content.

The drift chamber for IDEA is based on the drift chamber for the KLOE experiment [7] as well as a more recent version of it developed for the MEG2 experiment [3].

The drift chamber consists of a unique-volume with high granularity. It is foreseen to use a gas composed of 90 % of Helium and 10 % of isobutane (C_4H_{10}). It is composed of 112 co-axial layer with wires having an average stereo angle of 0.1 radians allowing for a longitudinal resolution of 1 mm. The square cell size varies between 12.0 mm and 14.5 mm. The parameters of the drift chamber for the IDEA detector are summarized in Table 1. The description of the simulation chain for the drift chamber using the FCCSW is described here-below.

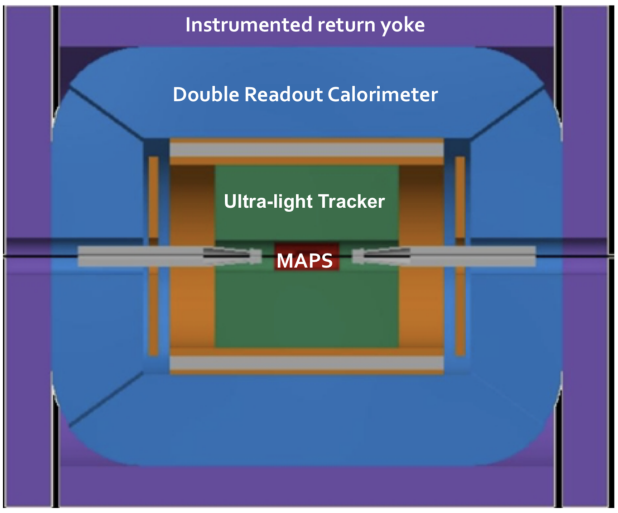

Figure 2: Schematic layout of the IDEA detector with the sub-detectors illustrated in different colors: vertex detector (red), drift chamber (green), pre-shower (orange), magnet (gray), calorimeter (blue), magnet yoke and muon system (violet).

Table 1: Parameters of the drift chamber for the IDEA detector

Length	4 m
Inner radius	0.345 m
Outer radius	2 m
Number of sensitive wires	56'448
Transverse resolution	0.1 mm
Longitudinal resolution	1 mm
Material content in radial direction	1.6%
Material content in the forward direction	5.0 %

3 Simulation with the FCC Software

The FCC Software (FCCSW) [1] is a common software for all FCC experiments. It is based on the Gaudi software framework [4] for parallel data processing, GEANT4 simulation toolkit [2] and the DD4hep detector description toolkit for high energy physics [8]. The FCCSW simulation pipeline is summarized in Fig. 3 and described here-below.

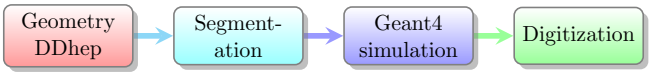

Figure 3: The FCCSW simulation chain.

3.1 Geometry description with DD4hep

First, the geometry of the detector is described using the DD4hep simulation framework. The current implementation of the detectors in the interaction region for the IDEA detector is shown in Fig. 4. The interaction region consists of a beam pipe, a shielding solenoid, a luminosity calorimeter, a vertex detector and a drift chamber. The geometry of the drift chamber is defined as layers of gas. In order to increase the simulation speed, the individual wires are not physically placed in the simulation software and the segmentation takes them into account.

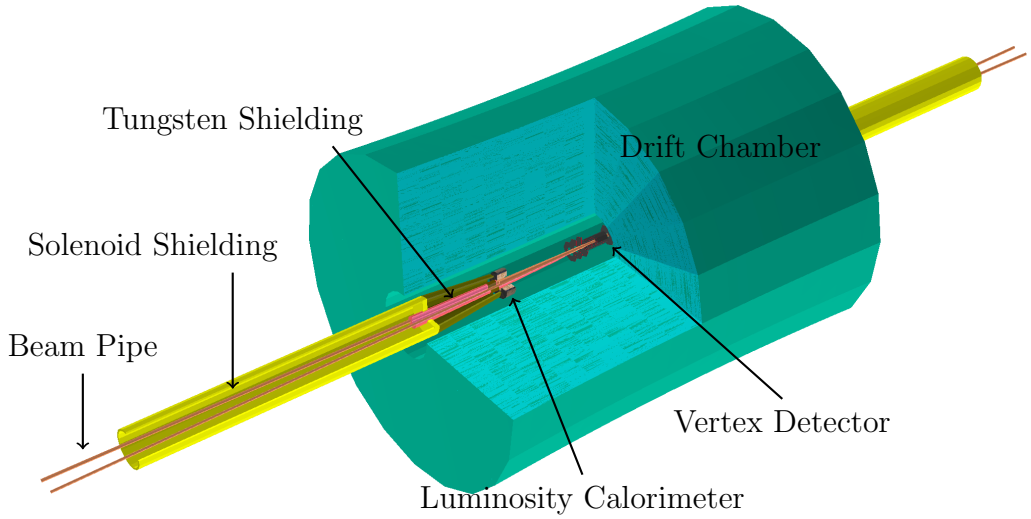

Figure 4: The detectors at the interaction region for the FCC-ee IDEA concept as implemented in FCCSW.

3.2 Segmentation

The segmentation of the sensitive gas detector contains the information on the positions of the wires in the detector. The segmentation for the first layer of the drift chamber is shown in Fig. 5. This reduces the running time by avoiding to place each wire volume individually. More details on the computation of the positions of the wires in the drift chamber are given in Appendix A.

The total number of wires as a function of the polar angle θ is illustrated in Fig. 6. In the barrel region, a high coverage is obtained by $\sim$ 112 wires in average. In the forward region, silicon disks are foreseen to improve the track angle coverage.

3.3 Geant4 simulation and digitization

GEANT4 simulates the passage of particles through matter. For the drift chamber simulation, a step size of 2 mm is chosen in order to step trough the gas volume and calculate the energy deposited. The ionization charge is then drifted to the nearest wire. This allows for calculating the drift time and therefore the signal in the wires. Once the contribution from

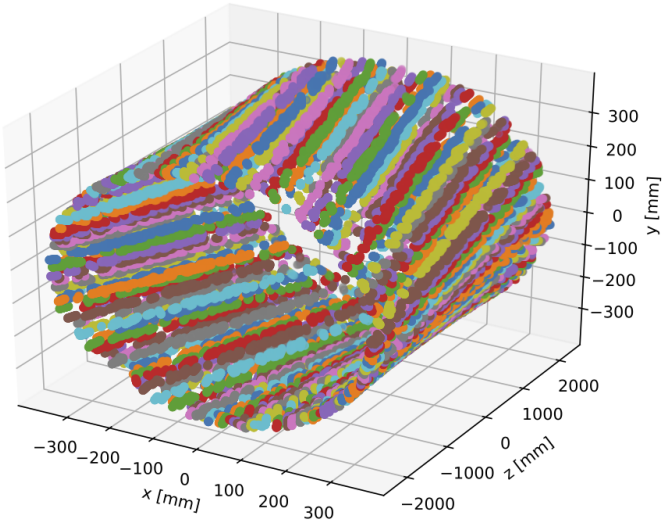

Figure 5: The segmentation of the first layer of the drift chamber.

each GEANT4 step is calculated, the digitization step regroups the energy deposited with a drift time smaller than the maximum drift time in the cell.

4 Impact of beam-induced backgrounds

Three main sources of beam-induced backgrounds at the FCC-ee experiment are: incoherent e^+e^- pairs, $\gamma\gamma \rightarrow$ hadrons and the synchrotron radiation. Each background source is studied below.

The incoherent e^+e^- pairs are generated from the strong electromagnetic force from the electron and positron bunches in the field of the opposite beam. This leads to the production of Beamstrahlung photons. The interactions of Beamstrahlung photons generate incoherent lepton pairs at low polar angles and mostly contained in the forward direction as shown in Fig. 7. The GUINEA-PIG [11] event generator has been used to generate the incoherent e^+e^- background particles at a $\sqrt{s}$ of 91.2 GeV and 365 GeV [5] and their impact on the drift chamber is simulated using the FCCSW. The occupancy of the drift chamber due to incoherent e^+e^- pairs as a function of the detector radius is shown in Fig. 8. In fact, the produced incoherent pairs have a low polar angle and only few of them reach the drift chamber. Most of the hits observed are due to the scattering of the e^+e^- pairs by interacting with the elements in the interaction region.

The $\gamma\gamma \rightarrow$ hadrons background is expected to have a very low impact on the drift chamber. The synchrotron radiation, dictates the design of the interaction region. It defines the beampipe radius and the design of the shielding (in Tungsten). Table 2 summarizes the occupancy in the drift chamber due to different sources of beam-induced backgrounds. The overall occupancy due to all backgrounds is as expected, with e^+e^- pair background having the highest impact. Based on previous experience with the MEG2 experiment, it can be deduced that the background does not pose problem for the reconstruction of the tracks using the drift chamber.

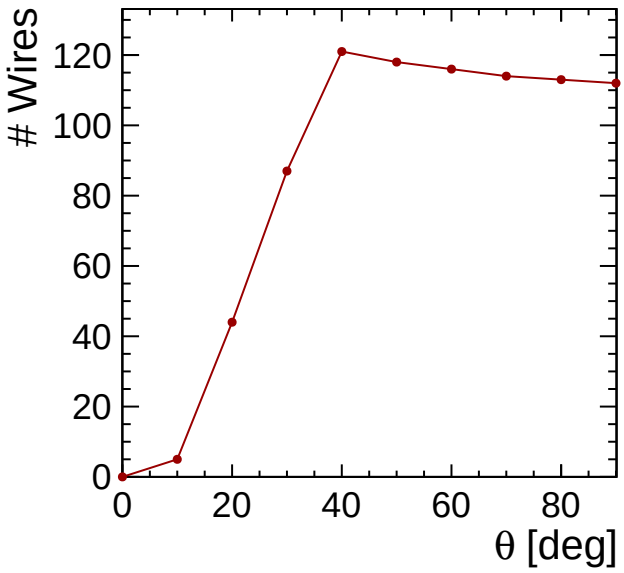

Figure 6: Total number of wires as a function of the polar angle θ (calculated using infinite momentum tracks from the origin).

Table 2: Average occupancy in the drift chamber due to beam-induced backgrounds.

Background	Average occupancy	
	$\sqrt{s} = 91.2$ GeV	$\sqrt{s} = 365$ GeV
e^+e^- pair background	1.1%	2.9%
$\gamma\gamma \to$ hadrons	0.001%	0.035%
Synchrotron radiation	negligible	0.2%

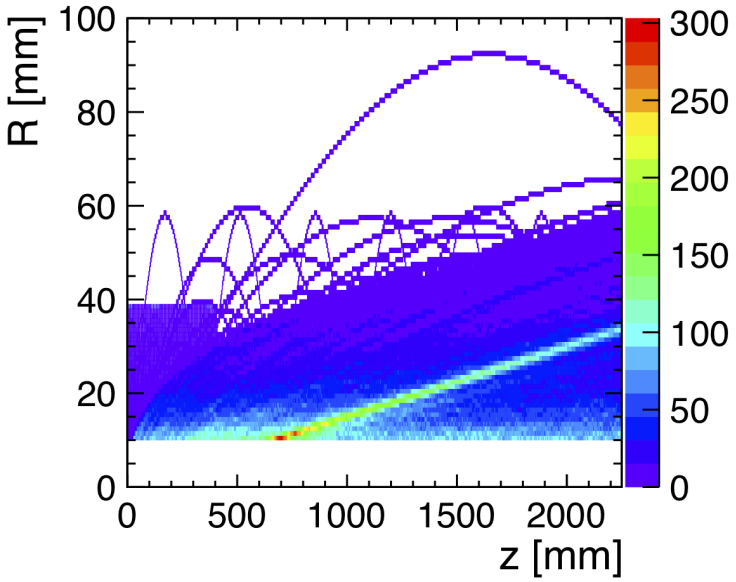

Figure 7: The trajectory of the e^+e^- pairs in a 2 T magnetic field.

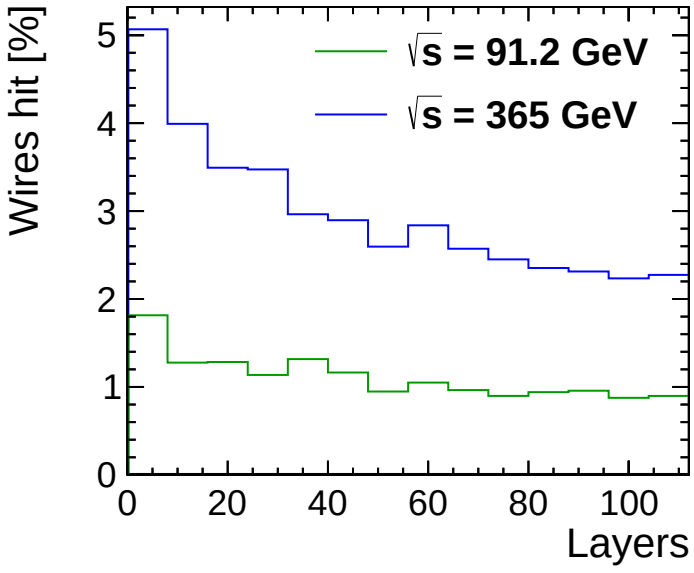

Figure 8: The percentage of wires hit due to e^+e^- pair background as a function of the layer radius averaged over 100 bunch crossings. For the Z stage ($\sqrt{s} = 91.2$ GeV), the readout latency is also taken into account by summing up the background over 4 bunch crossings.

5 Tracking

The drift chamber, with 112 layers of wires, provides high number of measurements which can be exploited for the track reconstruction.

The Hough Transform [10] has been investigated for the drift chamber and the results are presented in this chapter.

5.1 The Hough Transform

Initially invented for bubble chamber photographs [10], the Hough Transform is a feature extraction technique used in several fields such as image analysis, computer vision and digital image procession. It allows for the identification of lines as well as other shapes such as circles or ellipses.

5.1.1 Principle

The detection of straight lines is the most simple case for the Hough transformation. In the parameter space, lines are represented as a point (b, m) with Eq. (1).

$$y = m \cdot x + b \tag{1}$$

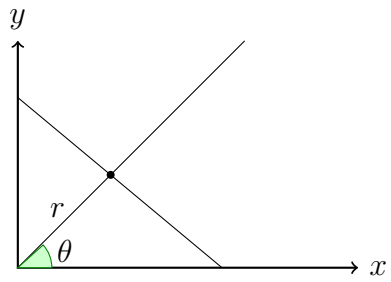

Figure 9: A line is represented as a point (b, m) in the parameter space or (r, θ) in the Hough space according to Eqs. (1) and (2).

With the presentation (b, m) in the parameter space, vertical lines pose problems for the unbounded slope parameter m. The Hesse normal form as described in Eq. (2) can be used as a solution to get around vertical lines, where r is the shortest distance from the origin to the line and θ is the angle between the x axis and the line connecting the origin with the closest point as illustrated in Fig. 9. The (r, θ) plane is referred to as the Hough Space.

$$r = x \cdot \cos(\theta) + y \cdot \sin(\theta) \tag{2}$$

Fig. 10 shows the Hough transformation applied to every point on a line. In the Hough space, all the points on the line are represented by a local maximum since they all have the same (r, θ) value.

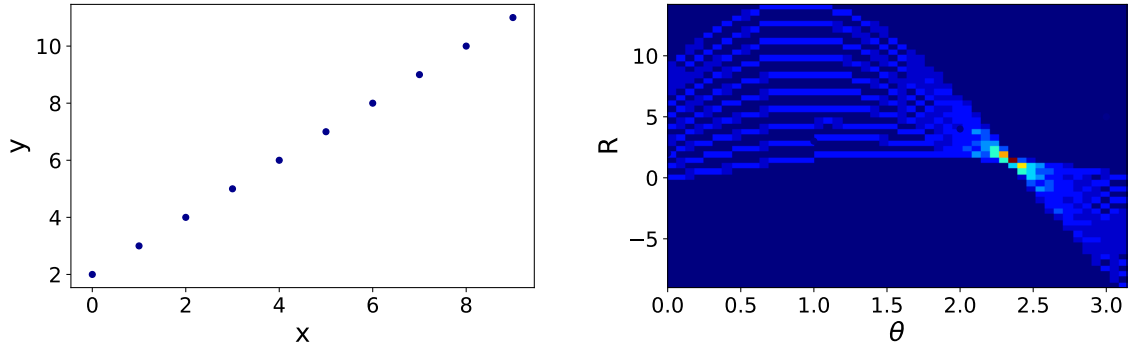

(a) Parameter space

(b) Hough space

Figure 10: A line as represented in the parameter and the Hough space.

5.1.2 Identification of circles

To identify the circle using the Hough transformation, two consecutive methods are applied: first the circle is transformed to a line (using the conformal transformation) and the Hough transformation is applied to the line. This method is explained in this part.

The track of a charged particle in a magnetic field follows a helicoidal trajectory. In the xy-plane, the hits follow a circular trajectory as described with Eq. (3) where (a, b) represent the center of the circle and R the radius of the circle.

$$(x - a)^2 + (y - b)^2 = R^2 \tag{3}$$

The Hough transformation gets better results when applied to lines. For this reason, first the conformal mapping [9] is first applied to map circular hits into lines using Eq. (4).

$$u = \frac{x}{x^2 + y^2}, \quad v = \frac{y}{x^2 + y^2} \tag{4}$$

The conformal mapping maps a circle to a line if and only if the circle passes from the origin or following the condition as described in Eq. (5) and the straight lines are described by Eq. (6).

$$a^2 + b^2 = R^2 \tag{5}$$

$$v = \frac{1}{2b} - u\frac{a}{b} \tag{6}$$

If the condition in Eq. (5) is not satisfied, some correction terms are needed for the transformation in Eq. (4) to transform circles into lines.

The Hough transformation is then applied to the straight lines using Eq. (7).

$$\rho = u \cdot cos(\phi) + v \cdot sin(\phi) \tag{7}$$

The radius of the circle R is connected the ρ parameter of the Hough transformation by Eq. (8).

$$R = \frac{1}{2 \cdot \rho} \tag{8}$$

Finally, the center of the circle is extracted from the Hough transformation using Eq. (9).

$$a = \frac{cos(\phi)}{2 \cdot \rho}, \quad b = \frac{sin(\phi)}{2 \cdot \rho} \tag{9}$$

Section 5.1.2 illustrates the conformal and Hough transformations as applied to circles. The local maxima in the Hough space, represents the circles in the xy-plane and their radius can be easily extracted using Eq. (8).

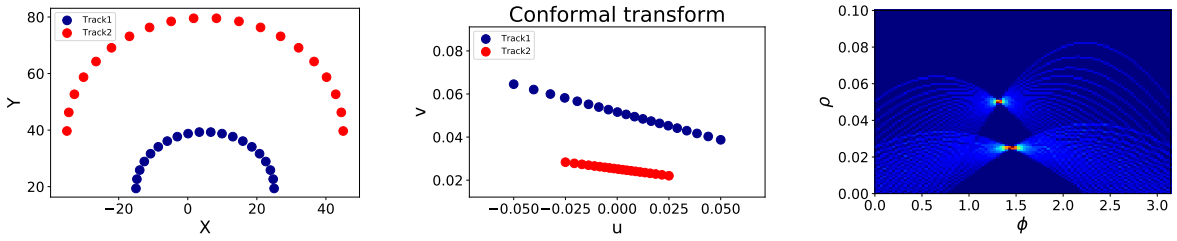

(a) (b) (c)

Figure 11: Circles (a) as represented after a conformal mapping (b) and after the Hough transformation (c).

The Hough transformation is a periodic function and the points in the $\rho - \theta$ plane are bounded by $\theta \in [0, 2\pi]$ and $\rho \in \left[-\sqrt{u^2+v^2}, \sqrt{u^2+v^2}\right]$. It is important to note that the points (θ, ρ) and $(\theta+\pi, -\rho)$ describe the same line. In the studies presented in this document, to remove the ambiguity, ρ is limited to positive values.

5.2 Identification of single tracks

The detection of single particle tracks simulated with FCCSW has been investigated.

Simulations using a 2.4 GeV muon particle gun have been done. In a 2 T magnetic field, the bending radius is 4 m. An event is displayed in Fig. 12.

Fig. 13 shows the conformal transformation to the (x-y) position of the simulated hits in the drift chamber and the hits are mapped to a line.

Finally the Hough transformation is applied to the conformal transform (Fig. 13) and the result is shown in Fig. 14. In the Hough space, all the hits corresponding to the same track are represented by a local maximum. Therefore, tracks are found by searching for local maxima in the Hough space. Also, the location of the maxima gives the information on the curvature of the track.

5.3 Finding local maxima in the Hough space

As seen in the previous chapter, the pattern recognition is performed by looking for local maxima in the Hough space. Since the drift chamber has 112 layers, a threshold is applied to select bins in the Hough space which have more than 112 entries. And to increase the

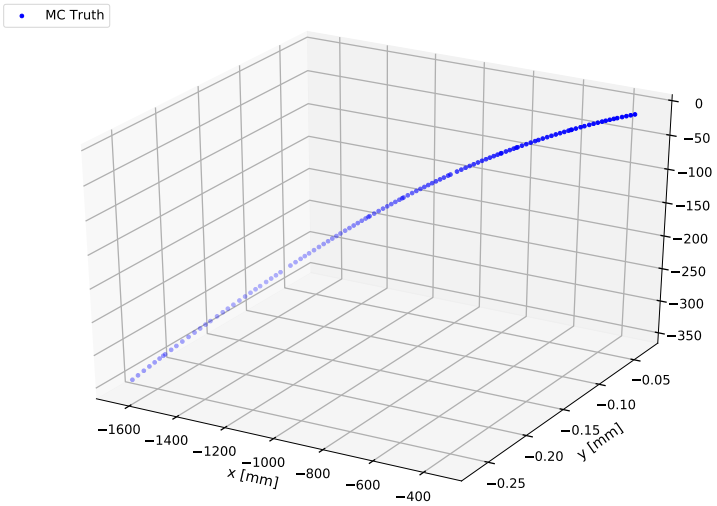

Figure 12: Simulated hits in the drift chamber for a 2.4 GeV muon in a 2 T magnetic field.

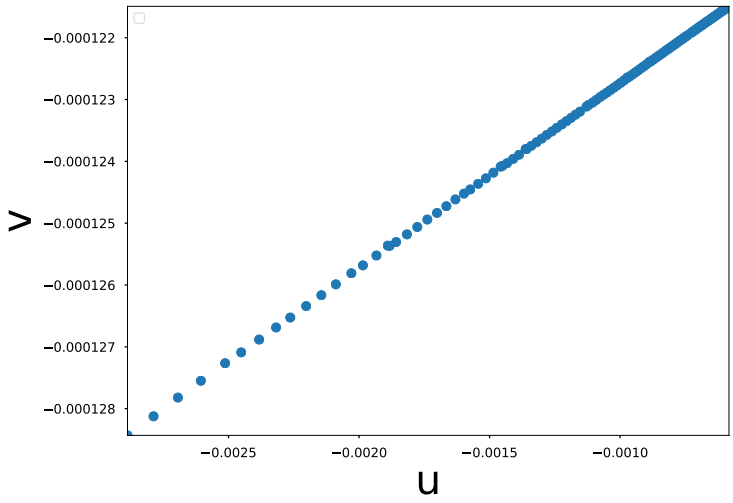

Figure 13: Conformal transformation for the hits as shown in Fig. 12.

accuracy, the neighboring bins around the bins with maximum hits are also investigated and they are clustered together. Fig. 15 shows the bins with at least 112 hits and also one cluster is found. The bending radius of the 2.4 GeV is correctly given by the Hough transformation.

The DBSCAN clustering algorithm[1] provided by the python library scikit-learn is used with a distance metric. With a distance of $\sqrt{2}\times$ bin size, the clusters' shapes are as illustrated in Fig. 16.

5.4 Incoherent e^+e^- background pairs

Fig. 17 shows the simulated hits in the drift chamber due to incoherent e^+e^- background pairs as described in Section 4.

[1]https://scikit-learn.org/stable/modules/generated/sklearn.cluster.DBSCAN.html

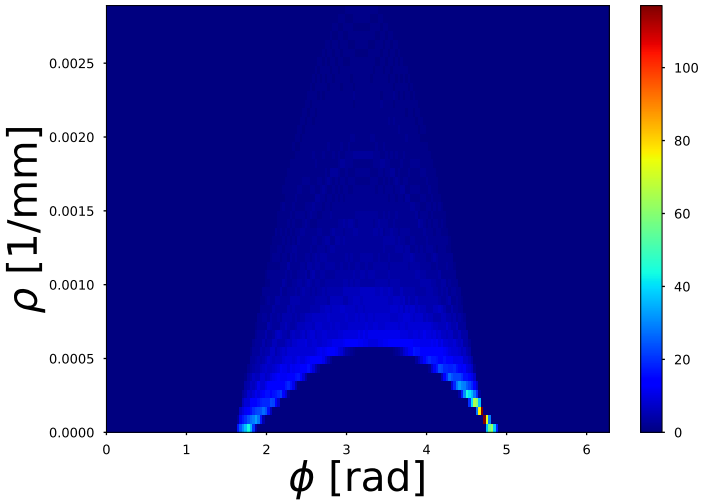

Figure 14: Hough transformation applied to the conformal transform as shown in Fig. 13.

The conformal transformation corresponding to the hits as shown in Fig. 17 is shown in Fig. 18. The conformal transform displays the tracks as lines.

Fig. 19 shows the Hough transformation of the background hits. The clustering algorithm finds 30 clusters. The confusion is due to the noisy environment. Also, the bin size and the threshold have a high impact on the number of clusters found. To reconstruct tracks in such a noisy environment, two solutions can be explored. First, the timing of the incoherent pairs can be explored to reduce hits with high timings. The second method would be to use the information from the seeding in the vertex detector and restrict the search for tracks in the Hough space based on the seeds.

5.5 Dijet events

The Hough transformation is also investigated for more complex events such as the decay of the Z-like boson into two light-quark dijets ($Z \rightarrow d\bar{d}$) for a center-of-mass energy of $\sqrt{s} = 91$ GeV. The hits in the drift chamber are displayed in Fig. 20.

The Hough transformation for such a complex event is shown in Fig. 21. As seen previously, the clustering can be very sensitive to the threshold and bin sizes in the Hough space. The information from the seeding of the vertex detector can improve the pattern recognition in the drift chamber.

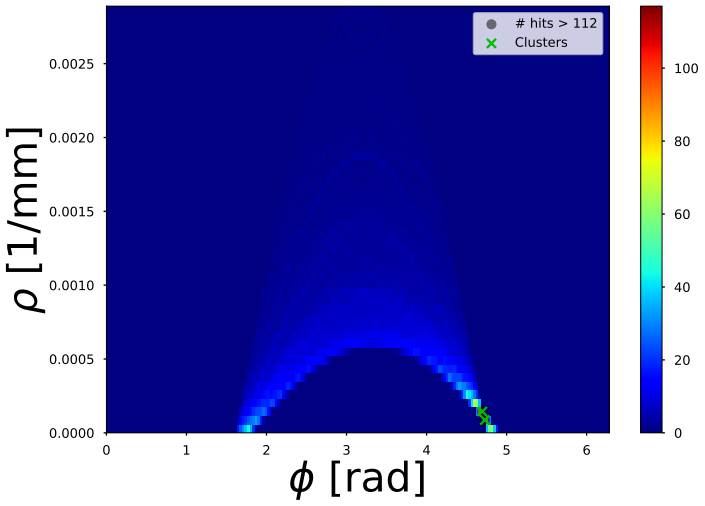

Figure 15: Finding the maxima in the Hough space of Fig. 14. The bins with more than 112 hits are highlighted and the clustering algorithm has found one cluster as shown in green.

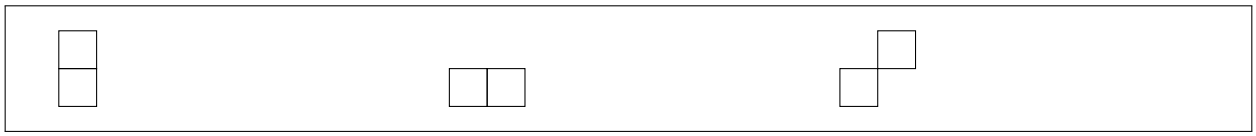

Figure 16: Configurations where the shapes are considered as a cluster with a distance criterion of $\sqrt{2}$.

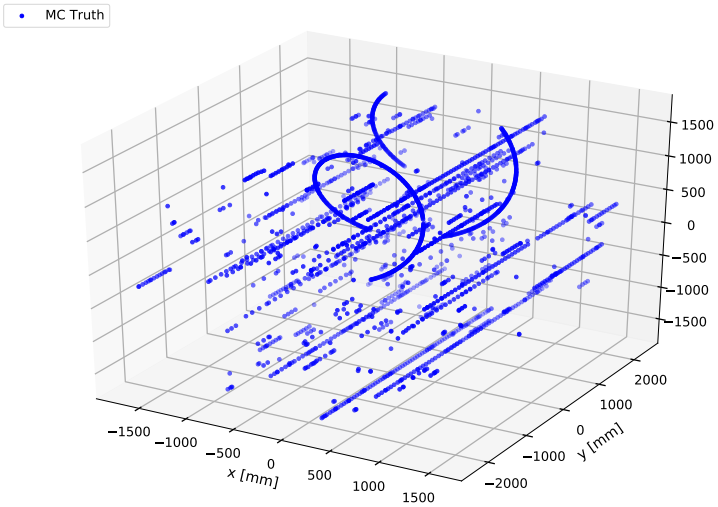

Figure 17: Display of the incoherent e^+e^- background hits in the drift chamber.

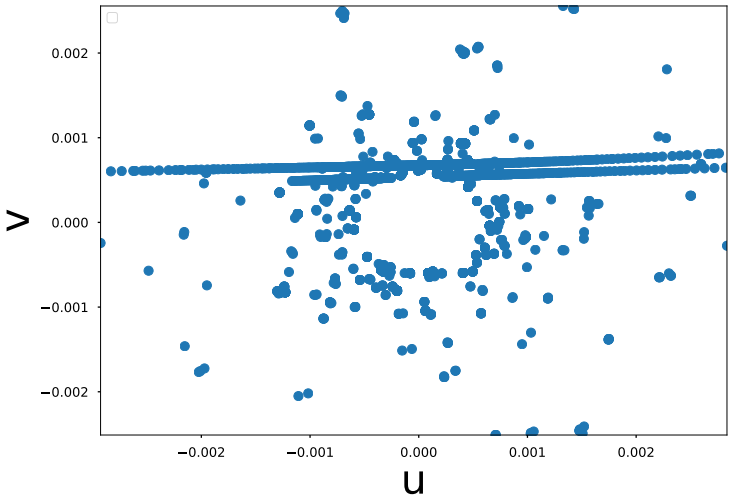

Figure 18: Display of the incoherent e^+e^- background hits in the drift chamber.

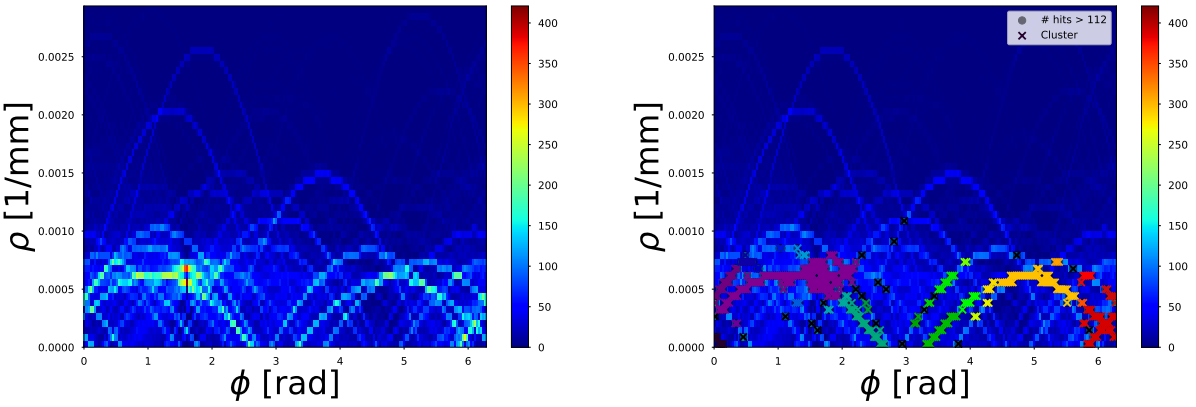

(a) (b)

Figure 19: (a) shows the e^+e^- background hits as represented in the Hough space. (b) shows the clusters found by the clustering algorithm.

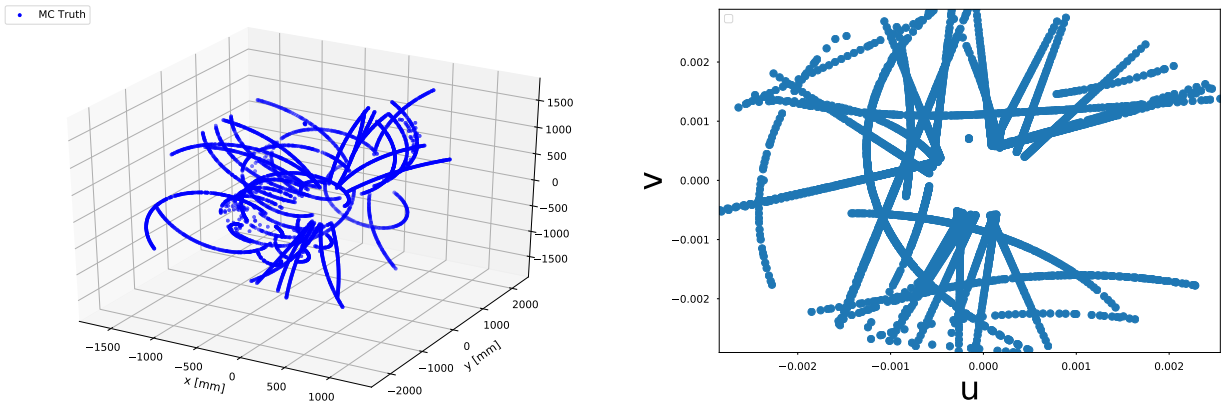

(a) (b)

Figure 20: (a) display of the hits in the drift chamber due to the decay $Z \to d\bar{d}$ at a center-of-mass energy of $\sqrt{s} = 91$ GeV. (b) displays the conformal transformation of such complex events.

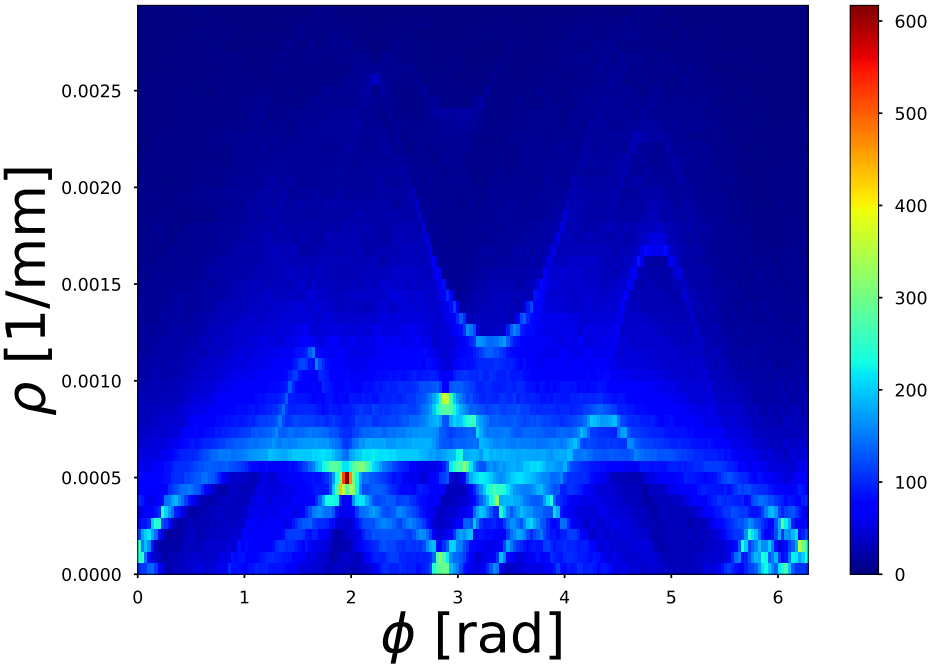

Figure 21: The Hough transformation corresponding to the $Z \to d\bar{d}$ decay.

6 Conclusions

The drift chamber for the IDEA detector concept has been implemented in the FCC common software (FCCSW). The full simulation chain has been implemented and validated. The impact of beam-induced backgrounds have been studied in simulations. The most important contribution belongs to the incoherent e^+e^- pair particles and it is important to study the feasibility of track reconstruction despite this background.

Since the drift chamber offers a high number of measurement layers, the Hough transformation could be a promising method for pattern recognition. The Hough transformation have been explored for the reconstruction of the tracks in the drift chamber. The parameters for this method need to be optimized. The combination of the seeding information coming from the vertex detector with the Hough transformation needs to be investigated and could provide high tracking efficiencies (even in the presence of beam-induced backgrounds).

A Segmentation

In this chapter, the equations used for placing the wires in the DCH are give. The same naming convention is as well used for the description of the geometry in FCCSW[2]. Fig. 22 shows a wire rotated with a stereo angle of ϵ. The angle $\alpha = 30°$ remains constant throughout all the layers.

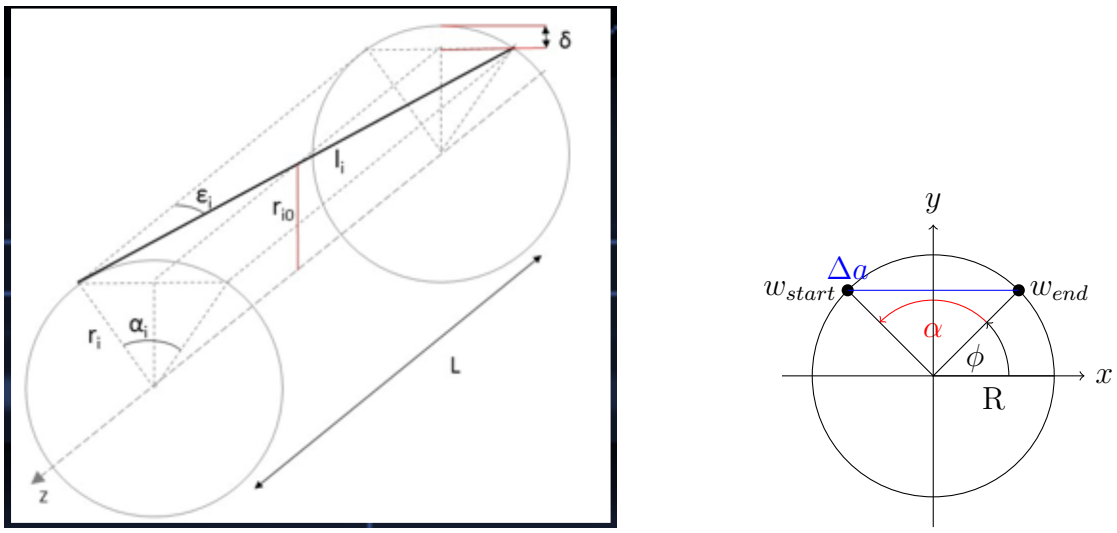

(a) (b)

Figure 22: (a) shows a wire as place in a 3D space and rotated with a stereo angle ϵ. (b) shows the projection of the wire in (a) into the xy-plane. α is the angle between the wire extremities in the xy-plane and it remains the same for all the layers ($\alpha = 30°$).

Eqs. (10) and (11) give the relationship between α and ϵ where L is the length of the drift chamber as shown in Fig. 22a.

$$\Delta a = L \cdot \tan(\epsilon) \tag{10}$$

$$\alpha = 2 \cdot \arcsin\left(\frac{L \cdot \tan(\epsilon)}{2 \cdot R}\right) \tag{11}$$

Eqs. (12) and (13) provide the coordinates of the extremities of the wires depending on the azimuthal angle ϕ where $|\phi_{start} - \phi_{end}| = \alpha$.

$$\vec{w}_{start} = \begin{pmatrix} R\cos(\phi_{start}) \\ R\sin(\phi_{start}) \\ L/2 \end{pmatrix} \tag{12}$$

$$\vec{w}_{end} = \begin{pmatrix} R\cos(\phi_{end}) \\ R\sin(\phi_{end}) \\ -L/2 \end{pmatrix} \tag{13}$$

[2] https://github.com/HEP-FCC/FCCSW/tree/master/Detector/DetFCCeeIDEA

The distance of the closest approach between a hit position $\vec{p}_{hit}$ and a wire is given by Eq. (14).

$$d = \frac{|(\vec{w}_{end} - \vec{w}_{start}) \times (\vec{w}_{start} - \vec{p}_{hit})|}{|(\vec{w}_{end} - \vec{w}_{start})|} \tag{14}$$

B Technical documentation

In this chapter, the a tutorial for setting up the simulation and the analysis of the IDEA detector is described. More information on the FCC software is available on the FCCSW webpage [1].

B.1 Installation of FCCSW from GitHub

First, fork the FCCSW repository on GitHub. Log in to LXPLUS SLC6 and clone your fork of the project.

Listing 1: Clone your fork of the FCCSW repository.

```
git clone https://github.com/[your-github-username]/FCCSW.git
cd FCCSW
```

Make sure to correctly set remote for the GitHub repository using the following guide[3]. To sync your fork with the upstream repository use the instructions given in this guide[4].

Setup the environment in order to build or use the software.

Listing 2: Setup the environment and compile.

```
source ./init.sh
make -j 12
```

B.2 Running FCCSW

In order to visualise the geometry of the FCCeeIDEA detector run the following command and the display is shown in Fig. 23.

Listing 3: Visualise the full geometry of the FCCeeIDEA detector.

```
./run geoDisplay -compact \
  Detector/DetFCCeeIDEA/compact/FCCee_DectEmptyMaster.xml \
  Detector/DetFCCeeIDEA/compact/FCCee_DectMaster.xml
```

The following script is used to run a simulation using particle gun from GEANT4. The output is written in a PODIO file. The output contains the energy deposits calculated by GEANT4 at each G4STEP.

Listing 4: Particle gun simulation.

```
./run fccrun.py Examples/options/geant_fullsim_fccee_pgun.py
```

B.3 Hit Reconstruction

The hits (or energy deposits calculated at each G4STEP) are then drifted to the corresponding wire. This step, outputs a ROOT file containing the wires hit (cellID, layerID and

[3] https://help.github.com/en/articles/configuring-a-remote-for-a-fork
[4] https://help.github.com/en/articles/syncing-a-fork

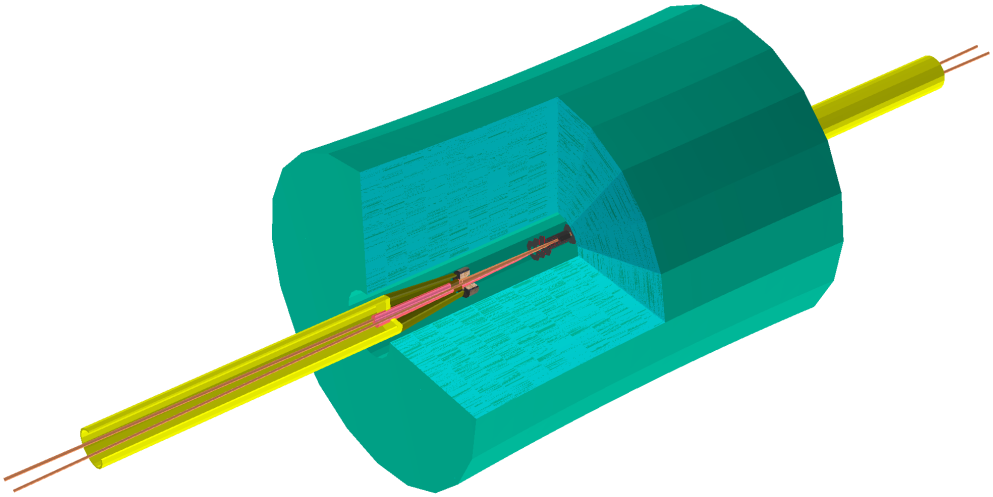

Figure 23: Visualisation of the FCCeeIDEA detector using FCCSW.

wireID), the Monte Carlo Truth positions, the distance of the closest approach of the track to the wire hit.

Listing 5: Reconstruction of the simulated hits for the drift chamber.

```
./run fccrun.py \
Reconstruction/RecDriftChamber/tests/options/mergeHits.py
```

B.4 Simulation of the pair backgrounds

For the simulation of incoherent e^+e^- pairs, the following command needs to be run. The input file is obtained from the GUINEA-PIG [11] simulation framework and it is written in the HEPEVT format. The output file is in PODIO format.

Listing 6: Simulation of the incoherent pair background.

```
./run fccrun.py Examples/options/geant_fullsim_fccee_hepevt.py \
--input=inFileName --outputfile=outFileName
```

The HEPEVT files can be found on eos for the top and Z stages.

Listing 7: Location of the background hits for the top stage.

```
/eos/experiment/fcc/ee/generation/GUINEA-PIG/top_hepevt
```

Listing 8: Location of the background hits for the Z stage.

```
/eos/experiment/fcc/ee/generation/GUINEA-PIG/Z_hepevt
```

B.5 Hough Transformation

The Hough Transformation is written in python and the code can be found on GitHub: https://github.com/nalipour/HoughTransform.

The instructions are given in the README.

References

[1] The Future Circular Collider Software Framework. http://fccsw.web.cern.ch/fccsw.

[2] S. Agostinelli et al. GEANT4: A Simulation toolkit. *Nucl. Instrum. Meth.*, A506:250–303, 2003.

[3] A. M. Baldini et al. The design of the MEG II experiment. *Eur. Phys. J.*, C78(5):380, 2018.

[4] G. Barrand et al. GAUDI - A software architecture and framework for building HEP data processing applications. *Comput. Phys. Commun.*, 140:45–55, 2001.

[5] Michael Benedikt, Alain Blondel, Olivier Brunner, Mar Capeans Garrido, Francesco Cerutti, Johannes Gutleber, Patrick Janot, Jose Miguel Jimenez, Volker Mertens, Attilio Milanese, Katsunobu Oide, John Andrew Osborne, Thomas Otto, Yannis Papaphilippou, John Poole, Laurent Jean Tavian, and Frank Zimmermann. Future Circular Collider. Technical Report CERN-ACC-2018-0057, CERN, Geneva, Dec 2018. Submitted for publication to Eur. Phys. J. ST.

[6] M. Bicer et al. First Look at the Physics Case of TLEP. *JHEP*, 01:164, 2014.

[7] Erika De Lucia. Status of the KLOE-2 Inner Tracker. *EPJ Web Conf.*, 166:00003, 2018.

[8] M. Frank, F. Gaede, and P. Mato. DD4hep: A Detector Description Toolkit for High Energy Physics Experiments. *J. Phys.: Conf. Ser.*, 513(AIDA-CONF-2014-004):022010, Oct 2013.

[9] M. Hansroul, H. Jeremie, and D. Savard. FAST CIRCLE FIT WITH THE CONFORMAL MAPPING METHOD. *Submitted to: Nucl. Instrum. Methods*, 1988.

[10] P. V. C. Hough. Machine Analysis of Bubble Chamber Pictures. *Conf. Proc.*, C590914:554–558, 1959.

[11] Daniel Schulte. Beam-Beam Simulations with GUINEA-PIG. Mar 1999.